

國立交通大學

電信工程研究所

碩士論文

頻率選擇性衰減通道之結合通道估計與
錯誤更正的四相相位偏移調變碼之設計

QPSK-modulated Code Design for Combined Channel
Estimation and Error Correction on a Frequency-selective
Fading Channel

研究生：陳詒欣

指導教授：陳伯寧

中華民國一百年六月

頻率選擇性衰減通道之結合通道估計與
錯誤更正的四相相位偏移調變碼之設計

QPSK-modulated Code Design for Combined Channel
Estimation and Error Correction on a Frequency-selective
Fading Channel

研究生：陳詒欣

Student：Yi-Hsin Chen

指導教授：陳伯寧 博士

Advisor：Dr. Po-Ning Chen



Submitted to Institute of Computer and Information Science
College of Electrical Engineering and Computer Science
National Chiao Tung University
in partial Fulfillment of the Requirements
for the Degree of
Master
in

Computer and Information Science

June 2011

Hsinchu, Taiwan, Republic of China

中華民國一百年六月

頻率選擇性衰減通道之結合通道估計與 錯誤更正的四相相位偏移調變碼之設計

學生：陳詒欣

指導教授：陳伯寧 博士

國立交通大學電信工程研究所碩士班

摘 要

在本篇論文，我們探討頻率選擇性衰減通道之結合通道估計與錯誤更正的四相相位偏移調變碼之設計。經過分析發現：在接收端對通道一無所知的情況下，QPSK 調變碼效能受相位干擾的影響比受振幅影響來的大。如果通道間的相位彼此是同步的，並建立一個調變碼的錯誤率聯集上界之閉合形式作為搜尋最佳化調變碼的標準。模擬結果顯示，根據提出的假設與搜尋標準，四相相位調變碼比起二相相位調變碼，效能上有所提升。

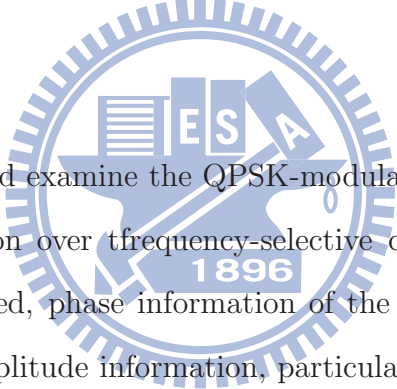
QPSK-modulated Code Design for Combined Channel Estimation and Error Correction on a Frequency-selective Fading Channel

Student: Yi-Hsin Chen Advisor: Po-Ning Chen

Institute of Communications Engineering

National Chiao Tung University

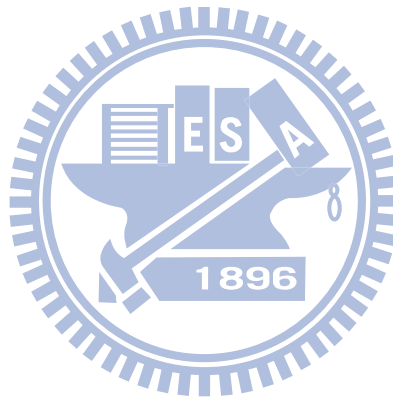
Abstract



In this thesis, we design and examine the QPSK-modulated codes for combined channel estimation and error protection over frequency-selective channels. We found that when QPSK modulation is considered, phase information of the channel coefficients is more essential than the respective amplitude information, particularly for the blind receiver we are interested in. Under the assumption that the unknown phases are synchronized among different channel taps, we establish a close-form-expressed union bound for the error performance and later use it as a criterion to search for the optimal code design. Our simulations show that the QPSK-modulated codes can provide an acceptable improvement over the BPSK-modulated codes.

Acknowledgements

I acknowledge Dr. Po-Ning Chen and Dr. Chia-Lung Wu for their encouragement and guidance. Without their advice, this work would not have been possible. I would also like to thank my dear laboratory mates. Finally, I give the great respect to my family for their continuing support.

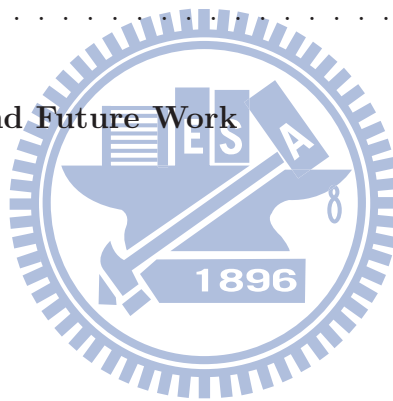


Contents

Chinese Abstract	i
Abstract	ii
Acknowledgements	iii
Contents	iv
List of Figures	vi
1 Introduction	1
1.1 Overview	1
1.2 Acronyms and Notations	3
2 Preliminaries	4
2.1 System Model	4
2.2 Code Design Criterion	6
2.3 Code Searching Algorithm	9
2.4 A Modified System Model Presumed in This Thesis	11



3	A Channel with Synchronized Phases Among Channel Taps: The Modified System Model	13
3.1	Impacts of Phase Distortions and Amplitude Distortions	14
3.2	PDFs of the Channel Coefficients of the Modified System Model	16
3.3	Approximate PDFs of the Channel Coefficients of the Modified System Model	17
3.4	The Decoding Criterion of the Modified System Model	19
4	The Simulation Results	21
4.1	System Settings	21
4.2	General Remarks	38
5	Conclusion Remarks and Future Work	39
	References	41



List of Figures

2.1	The modified system model	11
3.1	$E[X_n^4]$ with respect to f_{h_1, h_2} via Monte Carlo simulation.	19
4.1	The BERs of BPSK-modulated codes using decoder with no/phase/amplitude distortion information. The channel simulated is the Rayleigh-fading channel with $P = 1$. Here, the codeword lengths examined are $N = 4, 8, 12$, respectively.	24
4.2	The BERs of BPSK-modulated codes using decoder without/with phase distortion information. The channel simulated is the Rayleigh-fading channel with $P = 1$. Here, the codeword lengths examined are 4, 8, 12.	25
4.3	The BERs of QPSK-modulated codes using decoder with no/phase/amplitude phase distortion information. The channel simulated is the Rayleigh-fading channel with $P = 1$. Here, the codeword lengths examined are $N = 4, 8, 12$	26
4.4	The BERs of QPSK-modulated codes using decoder without/with phase distortion information. The channel simulated is the Rayleigh-fading channel with $P = 1$. Here, the codeword lengths examined are $N = 4, 8, 12$	27

4.5	The BERs of BPSK-modulated codes using decoder without/with phase distortion information. The channel simulated is the multi-path Rayleigh-fading channel with $P = 2$. Here, the codeword lengths examined are $N = 4, 8, 12$.	28
4.6	The BERs of BPSK-modulated codes using decoder without/with phase distortion information. The channel simulated is the multi-path Rayleigh-fading channel with $P = 2$. Here, the codeword lengths examined are $N = 4, 8, 12$.	29
4.7	The BERs of QPSK-modulated codes using decoder without/with phase distortion information. The channel simulated is the multi-path Rayleigh-fading channel with $P = 2$. Here, the codeword lengths examined are $N = 4, 8, 12$.	30
4.8	The BERs of QPSK-modulated codes using decoder without/with phase distortion information. The channel simulated is the multi-path Rayleigh-fading channel with $P = 2$. Here, the codeword lengths examined are $N = 4, 8, 12$.	31
4.9	The BERs of BPSK-modulated and QPSK-modulated codes using decoder without any information on the channels. The channel simulated is the multi-path Rayleigh-fading channel with $P = 2$, for which the phases of two channel taps are independent. Here, the codeword lengths examined are $N = 4, 8, 12$.	32
4.10	The BERs of BPSK-modulated and QPSK-modulated codes using decoder without any information on the channels. The channel simulated is the multi-path Rayleigh-fading channel with $P = 2$, for which the phases of two channel taps are independent. Here, the codeword lengths examined are $N = 4, 8, 12$.	33

4.11	The BERs of BPSK-modulated and QPSK-modulated codes using decoder with the information that the phases of two channel taps are synchronized. The channel simulated is the multi-path fading with $P = 2$, for which the phases of two channel taps are also synchronized. Here, the codeword lengths examined are $N = 4, 8, 12$	34
4.12	The BERs of BPSK-modulated and QPSK-modulated codes using decoder with the information that the phases of two channel taps are synchronized. The channel simulated is the multi-path fading with $P = 2$, for which the phases of two channel taps are also synchronized. Here, the codeword lengths examined are $N = 4, 8, 12$	35
4.13	The BERs of the $(N, N/2)$ and $(N, N/4)$ BPSK-modulated codes using decoder with the information that the phases of two channel taps are synchronized. The channel simulated is the multi-path fading with $P = 2$, for which the phases of two channel taps are also synchronized. Here, the codeword lengths examined are $N = 4, 8, 12$	36
4.14	The BERs of the (N, N) , $(N, N/2)$, $(N, N/4)$ QPSK-modulated codes using decoder with the information that the phases of two channel taps are synchronized. The channel simulated is the multi-path fading with $P = 2$, for which the phases of two channel taps are also synchronized. Here, the codeword lengths examined are $N = 4, 8, 12$	37

Chapter 1

Introduction

1.1 Overview

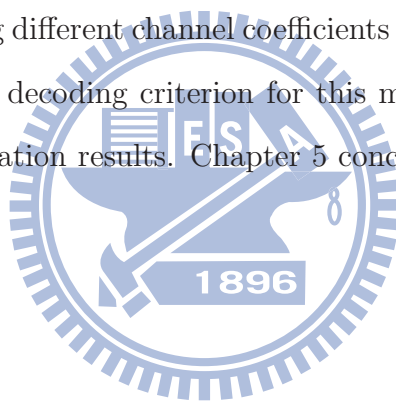
Traditionally, in a communication system over a fading environment, channel estimation, channel equalization and error correction are carried out at the receiver in sequence. The good performance of this typical system then relies heavily on an accurate estimate of channel coefficients. As such, a known training sequence of a nontrivial length has to be employed. However, even with a long training sequence, it might still be hard to yield an acceptably good estimate for channel coefficients under severe channel fades.

In 2002, Skoglund *et al.* [1] proposed combining channel estimation and equalization with the error correction and found the optimal non-linear binary code for channels with unknown parameters by computer search. Simulations showed that the computer searched code outperforms the Golay (23,12) code extended with one known pilot by 1.3 dB at $\text{WER} = 10^{-2}$. At such background, this thesis will continue the quest along this research line, and focus on the code design based on BPSK/QPSK modulations for combined channel estimation and error correction over a fading channel.

In particular, we attempt to design the QPSK modulated codes, rather than the BPSK modulated codes as in [1], because we wish to improve the transmission rate. The pre-

liminary simulations however indicate that the receiver may need to know the phases in order to achieve an acceptable performance for QPSK modulated codes. Yet, we found that by adding a simple assumption such that the phases among different channel coefficients are identical although they are unknown, the performance of the blind receiver can be significantly improved. The problem of this simple assumption is that it does not give a close-form-expressed union bound that can be conveniently used as the criterion for code search. An approximation will then be proposed and showed to be useful in code search.

The remaining parts of the thesis are organized as follows. Chapter 2 introduces the background knowledge about the code design for combined channel estimation and error correction, and gives a modified system model used in subsequent chapters. Chapter 3 assumes that the phases among different channel coefficients are synchronized (i.e., identical), and derives the optimal blind decoding criterion for this modified system model. Chapter 4 presents and discusses simulation results. Chapter 5 concludes the thesis and remarks on the possible future work.



1.2 Acronyms and Notations

The acronyms and some common identifiers used in this thesis are listed as follows.

BER bit error rate

WER word error rate

ML maximum-likelihood

SNR signal-to-noise ratio

N block length of a code, i.e., the number of symbols in a codeword

K number of bits in an information sequence to be encoded

P number of channel paths or taps

L $L = N + P - 1$ is the sum of a codeword length plus the minimum guard interval without interblock interference

The following notations are used in this thesis.

Symbol	Meaning
\mathbf{v}	a vector (<i>The following notations are simple representative examples. Similar notations are applied to other alphabets.</i>)
v_k	the k -th component of a vector \mathbf{v}
$\ \mathbf{v}\ ^2$	the norm of a vector \mathbf{v}
\mathbb{X}	a matrix
$x_{k,\ell}$	the element of a matrix \mathbb{X} at row k and column ℓ
\mathbb{X}^T	transpose of a matrix \mathbb{X}
\mathbb{X}^H	Hermitian transpose of a matrix \mathbb{X}
\mathbb{I}_L	the $L \times L$ identity matrix
i	the imaginary unit

Chapter 2

Preliminaries

In this chapter, we provide the background knowledge about the code design for combined channel estimation and error correction. Specifically, Section 2.1 introduces the typical system model considered in the non-coherent system literature. Section 2.2 talks about the design criterion that is usually adopted in the literature. Section 2.3 gives the algorithm that will be used for code searching. Section 2.4 concludes this chapter by presenting a modified system model that will be used in the subsequent chapters.

2.1 System Model

The system model introduced in this section is precisely the one adopted in [1] except that the code symbols are not restricted to $\{-1, +1\}$ but can be extended to $\{-1, +1, -i, +i\}$. In the system considered therein, a length- N codeword $\mathbf{b} = [b_1, \dots, b_N]^T$ of an (N, K) block code \mathcal{C} is transmitted through a quasi-static block fading channel of memory order $(P - 1)$; hence, the channel coefficients can be expressed by a P -by-1 vector \mathbf{h} . Other than the fading effect, the system suffers an additive white Gaussian noise. This gives a system model as

$$\mathbf{y} = \mathbb{B}\mathbf{h} + \mathbf{n}$$

where

$$\mathbb{B} \triangleq \begin{bmatrix} b_1 & 0 & \cdots & 0 \\ \vdots & b_1 & \ddots & \vdots \\ b_N & \vdots & \ddots & 0 \\ 0 & b_N & \ddots & b_1 \\ \vdots & \ddots & \ddots & \vdots \\ 0 & 0 & \cdots & b_N \end{bmatrix}_{L \times P} \quad \text{with every } b_i \in \{\pm 1, \pm i\}, \quad (2.1)$$

\mathbf{n} is an $L \times 1$ zero-mean complex Gaussian vector with covariance matrix $\sigma^2 \mathbb{I}_L$, and $L = N + P - 1$. Here, we adopt the notational convention by denoting the L -by- L identity matrix by \mathbb{I}_L .

Note that as similar to [1], $(P - 1)$ should be regarded as an upper bound of the true memory order and is the only information that both the transmitter and receiver priorly know. In addition, the channel coefficient vector \mathbf{h} , although unknown to both transmitter and receiver, remains *constant* during the transmission of a codeword. Under these two assumptions, the optimal decoder is the so-called joint maximum-likelihood (JML) decoder:

$$(\hat{\mathbf{b}}, \hat{\mathbf{h}}) = \arg \min_{(\mathbf{b}, \mathbf{h}) \in \mathcal{C} \times \mathbb{C}^P} \|\mathbf{y} - \mathbb{B}\mathbf{h}\|^2,$$

where \mathcal{C} is the set of all codewords, and \mathbb{C} consists of all complex numbers.

For a given codeword \mathbf{b} , it can be derived that the optimal estimation $\hat{\mathbf{h}}$ that minimizes $\|\mathbf{y} - \mathbb{B}\mathbf{h}\|^2$ is equal to

$$\hat{\mathbf{h}} = (\mathbb{B}^H \mathbb{B})^{-1} \mathbb{B}^H \mathbf{y},$$

where superscript “ H ” denotes the Hermitian transpose operation. Hence, the JML estimator of the transmitted codeword is given by

$$\begin{aligned} \hat{\mathbf{b}} &= \arg \min_{\mathbf{b} \in \mathcal{C}} \|\mathbf{y} - \mathbb{B}(\mathbb{B}^H \mathbb{B})^{-1} \mathbb{B}^H \mathbf{y}\|^2 \\ &= \arg \min_{\mathbf{b} \in \mathcal{C}} \|\mathbf{y} - \mathbb{P}_B \mathbf{y}\|^2, \end{aligned} \quad (2.2)$$

where $\mathbb{P}_B \triangleq \mathbb{B}(\mathbb{B}^H \mathbb{B})^{-1} \mathbb{B}^H$, which can be pre-computed and stored during the decoding

process. Notably, \mathbb{P}_B and \mathbb{B} (equivalently, \mathbf{b}) are not one to one correspondence unless the first bit is fixed. For this reason, we will fix the first bit as $b_1 = 1$ in our code design.

2.2 Code Design Criterion

In this thesis, we attempt to search an (N, K) code \mathcal{C} by simulated annealing, which minimizes the union bound of the average block error probability P_e defined by

$$\begin{aligned} P_e &\triangleq 2^{-K} \sum_{\mathbf{b} \in \mathcal{C}} \Pr \left(\hat{\mathbf{b}} \neq \mathbf{b} \mid \mathbf{b} \text{ transmitted} \right) \\ &= 2^{-K} \sum_{i \in \mathcal{J}} \Pr \left(\hat{\mathbf{b}} \neq \mathbf{b}(i) \mid \mathbf{b}(i) \text{ transmitted} \right), \end{aligned}$$

where, for convenience, we denote by \mathcal{J} the set of indices of codewords in \mathcal{C} . The union bound of P_e , which we adopt in this thesis, is given by

$$P_e \leq 2^{-K} \sum_{i \in \mathcal{J}} \sum_{j \in \mathcal{J}, j \neq i} p_{j|i}, \quad (2.3)$$

where $p_{j|i}$ is the pairwise error probability (PEP) defined by

$$p_{j|i} \triangleq \Pr \left(\hat{\mathbf{b}} = \mathbf{b}(j) \mid \mathbf{b}(i) \text{ transmitted} \right). \quad (2.4)$$

The PEP, according to (2.2), can be represented as

$$\begin{aligned} p_{j|i} &= \Pr \left(\|\mathbf{y}(i) - \mathbb{P}_B(j)\mathbf{y}(i)\|^2 < \|\mathbf{y}(i) - \mathbb{P}_B(i)\mathbf{y}(i)\|^2 \right) \\ &\quad + \frac{1}{2} \Pr \left(\|\mathbf{y}(i) - \mathbb{P}_B(j)\mathbf{y}(i)\|^2 = \|\mathbf{y}(i) - \mathbb{P}_B(i)\mathbf{y}(i)\|^2 \right), \end{aligned} \quad (2.5)$$

where $\mathbb{P}_B(i) = \mathbb{B}(i)(\mathbb{B}^H(i)\mathbb{B}(i))^{-1}\mathbb{B}^H(i)$ is the projection matrix onto the column space of $\mathbb{B}(i)$ and the received vector $\mathbf{y}(i) = \mathbb{B}(i)\mathbf{h} + \mathbf{n}$ is now complex Gaussian distributed with mean $\mathbf{m}_y(i) = \mathbb{B}(i)\mathbf{m}_h$ and covariance matrix $\mathbb{S}_y(i) = \mathbb{B}(i)\mathbb{S}_h\mathbb{B}^H(i) + \sigma_n^2\mathbb{I}_L$. Since $\mathbf{y}(i)$ has density and since our code book satisfies $\mathbb{P}_B(i) \neq \mathbb{P}_B(j)$ for $i \neq j$, the second term in (2.5) is equal to zero when $i \neq j$. Thus,

$$p_{j|i} = \Pr \left(\|\mathbf{y}(i) - \mathbb{P}_B(j)\mathbf{y}(i)\|^2 < \|\mathbf{y}(i) - \mathbb{P}_B(i)\mathbf{y}(i)\|^2 \right). \quad (2.6)$$

By defining $\mathbb{Q}(j, i) \triangleq \mathbb{P}_B(j) - \mathbb{P}_B(i)$, the PEP in (2.6) can be rewritten as

$$p_{j|i} = \Pr(\mathbf{y}^H(i)\mathbb{Q}(j, i)\mathbf{y}(i) > 0). \quad (2.7)$$

It is reasonable to assume that $\sigma_n^2 > 0$; hence, the real and symmetric matrix $\mathbb{S}_y(i)$ is positive definite and can be factorized to $\mathbb{S}_y(i) = \mathbb{S}_y^{1/2}(i)\mathbb{S}_y^{1/2}(i)$. We then consider the real and symmetric $L \times L$ matrix

$$\mathbb{S}_y^{1/2}(i)\mathbb{Q}(j, i)\mathbb{S}_y^{1/2}(i),$$

and decompose it into sum of outer products of orthonormal eigenvectors $\{\mathbf{q}_n\}_{n=1}^L$ with eigenvalues as multiplicative coefficients $\{\lambda_n\}_{n=1}^L$, i.e.,

$$\mathbb{S}_y^{1/2}(i)\mathbb{Q}(j, i)\mathbb{S}_y^{1/2}(i) = \sum_{n=1}^L \lambda_n \mathbf{q}_n \mathbf{q}_n^T. \quad (2.8)$$

Without loss of generality, we index these eigenvalues in descending order, namely,

$$\lambda_1 \geq \lambda_2 \geq \dots \geq \lambda_L. \quad (2.9)$$

By this, together with (2.8), we get

$$\begin{aligned} \mathbf{y}^H(i)\mathbb{Q}(j, i)\mathbf{y}(i) &= (\mathbb{S}_y^{-1/2}(i)\mathbf{y}(i))^H \mathbb{S}_y^{1/2}(i)\mathbb{Q}(j, i)\mathbb{S}_y^{1/2}(i) (\mathbb{S}_y^{-1/2}(i)\mathbf{y}(i)) \\ &= \sum_{n=1}^L \lambda_n |\mathbf{q}_n^T \mathbb{S}_y^{-1/2}(i)\mathbf{y}(i)|^2 \\ &= \sum_{n=1}^L \lambda_n |X_n|^2, \end{aligned} \quad (2.10)$$

where

$$X_n \triangleq \mathbf{q}_n^T \mathbb{S}_y^{-1/2}(i)\mathbf{y}(i)$$

is complex Gaussian distributed with mean

$$m_x(n) = \mathbf{q}_n^T \mathbb{S}_y^{-1/2}(i)\mathbb{B}(i)\mathbf{m}_h$$

and variance $\sigma_{X_n}^2 = 1$. This leads to that $\{|X_n|^2\}_{n=1}^L$ are noncentral χ^2 -variables. Because the eigenvectors $\{\mathbf{q}_n\}_{n=1}^L$ are orthonormal, $\{X_n\}_{n=1}^L$ are independent and identically distributed random variables. With (2.7) and (2.10), we conclude that $p_{j|i}$ is the probability that the weighted sum of these noncentral χ^2 -variables is larger than zero.

We can further re-formulate (2.10) and obtain

$$\sum_{l=1}^{\bar{L}} \bar{\lambda}_l \cdot \chi^2(2k_l; \eta_l), \quad (2.11)$$

where \bar{L} is the number of distinct eigenvalues in $\{\lambda_n\}_{n=1}^L$, k_l is the multiplicity of the eigenvalue $\bar{\lambda}_l$, and $\chi^2(2k; \eta)$ stands for a noncentral χ^2 -variable with $2k$ degrees of freedom and noncentrality parameter η . Condition (2.9) immediately gives

$$\bar{\lambda}_1 > \bar{\lambda}_2 > \dots > \bar{\lambda}_{\bar{L}}.$$

Denote for convenience the random variable

$$Y_{i,j} \triangleq \mathbf{y}^H(i) \mathbf{Q}(j, i) \mathbf{y}(i)$$

with its characteristic function $\phi_{i,j}(t) = E[e^{itY_{i,j}}]$. Since $Y_{i,j}$ consists of \bar{L} independent χ^2 -variable, $\phi_{i,j}(t)$ is given by

$$\phi_{i,j}(t) = \prod_{l=1}^{\bar{L}} (1 - 2i\bar{\lambda}_l t)^{-k_l/2} \exp\left(i \sum_{r=1}^{\bar{L}} \frac{\eta_r \bar{\lambda}_r t}{1 - 2i\bar{\lambda}_r t}\right). \quad (2.12)$$

We then note that $p_{j|i}$ can be expressed in terms of $\phi_{i,j}(t)$ according to

$$p_{j|i} = \frac{1}{2\pi} \int_0^\infty \left[\int_{-\infty}^\infty \phi_{i,j}(t) e^{-ity} dt \right] dy. \quad (2.13)$$

In general, (2.13) dose not have a closed-form formula. Nevertheless, when a codeword is transmitted over the Rayleigh fading channel with $\mathbf{m}_h = 0$, the closed-form expression exists. By assuming that $\bar{\lambda}_p > 0 \geq \bar{\lambda}_{p+1}$ and letting $q \triangleq \sum_{l=1}^{\bar{L}} k_l$, (2.13) can be solved [3] as

$$p_{j|i} = \sum_{l=1}^p \frac{1}{(k_l - 1)!} \left[\frac{\partial^{k_l-1}}{\partial x^{k_l-1}} F_l(x) \right]_{x=\bar{\lambda}_l}, \quad (2.14)$$

where

$$F_l(x) = x^{q-1} \prod_{1 \leq r \leq L, r \neq l} (x - \bar{\lambda}_r)^{-k_r}.$$

Consequently, under Rayleigh fading channel with $\mathbf{m}_h = 0$, from [3], the design criterion (2.3) can be evaluated via (2.14).

2.3 Code Searching Algorithm

In this subsection, we will introduce the simulated annealing algorithm and later will apply it for code searching.

A typical simulated annealing algorithm follows the below procedure:

Choose initial code \mathcal{J} and initial temperature T .

REPEAT

REPEAT

Chose another code \mathcal{J}' .

Set $\Delta\epsilon = \epsilon(\mathcal{J}') - \epsilon(\mathcal{J})$.

IF ($\Delta\epsilon < 0$)

THEN Set $\mathcal{J} = \mathcal{J}'$.

ELSE With probability p , set $\mathcal{J} = \mathcal{J}'$.

UNTIL (Reach a certain number of energy drops or too many iterations.)

Set $T = \alpha T$.

UNTIL (Reach the targeted freezing temperature.)

The detail of the above algorithm, specifically for our code search, is given below.

- The initial code \mathcal{J} consists of the first 2^K elements of all possible candidates, listing

in alphabetical order.

- This system is heated initially and then cooled down, for which the initial temperature is $T = 10^7$ and the targeted freezing temperature is 10^{-7} .
- In the inner loop, a random code perturbation is implemented. The new code \mathcal{J}' is almost the same as \mathcal{J} . The only difference between them is that one of the codewords in \mathcal{J} , drawn in random, will be replaced by a randomly picked word originally outside \mathcal{J} .
- The energy function $\epsilon(\cdot)$ of this system is the union bound in (2.3) without the multiplicative constant 2^{-K} , i.e.,

$$\epsilon(\mathcal{J}) \triangleq \sum_{i \in \mathcal{J}} \sum_{j \in \mathcal{J}, j \neq i} p_{j|i},$$

which can be evaluated via (2.14).

- When $\Delta\epsilon < 0$, the code \mathcal{J}' performs better (i.e., has a smaller union bound) and hence the new code \mathcal{J}' will substitute the original one \mathcal{J} ; such case will be referred to as \mathcal{A} -perturbation.

To avoid falling into a local minima, replacing the old code \mathcal{J} by the new code \mathcal{J}' is still conducted with probability $p = \exp(-\frac{\Delta\epsilon}{T})$ when $\Delta\epsilon \geq 0$. Such a replacement when it is conducted will be referred to as \mathcal{B} -perturbation.

- The inner loop ends if more than 5 \mathcal{A} -perturbations occur, or more than 500 \mathcal{B} -perturbations is reached.
- Following [1], we set $\alpha = 0.995$.

We conclude the subsection by pointing out that after the code is selected, the encoder will map the uniformly distributed information messages to the codewords in alphabetical order.

In other words, the first information sequence in its own alphabetical order will correspond to the first code word also in its respective alphabetical order, the second information sequence will be mapped to the second codeword, etc. Simulations show that such simple mapping will result in a BER that is comparable to the best mapping obtained by simulated annealing [4]; hence, we adopt this simple alphabetical-order-based mapping for ease of our system implementation.

2.4 A Modified System Model Presumed in This Thesis

In reality, the channel coefficients $\mathbf{h} = [h_1, h_2, \dots, h_P]^T$ may not be totally independent. As an example for a channel with two taps as shown in Figure 2.1, their phases (that incur from their delays in signal traveling over two different major paths) should have constant difference. So the traditionally convenient assumption that h_1 and h_2 are independent complex variables may not be reasonable. In particular, such assumption would make the noncoherent detection of the QPSK signals somehow infeasible. Thus, we modify the system model introduced in Section 2.1 in this subsection (and also in the sequel) by assuming that the phases of all channel taps have constant difference while their amplitudes remain independent. For simplicity, we further assume these differences are all zero.

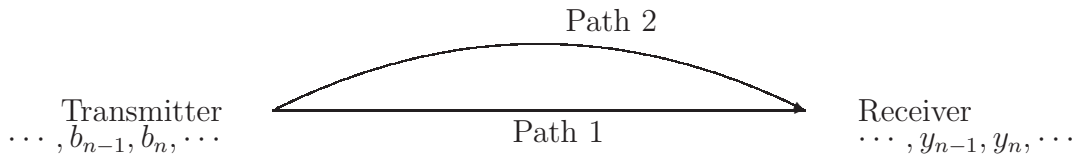


Figure 2.1: The modified system model

Denote by a_i the amplitude distortion and by θ_i the phase distortion of path i . For

convenience of its description, we let $P = 2$. With the new setting, the reception at time n can be obtained as

$$\begin{aligned} y_n &= h_1 \cdot b_n + h_2 \cdot b_{n-1} \\ &= a_1 e^{i\theta} \cdot b_n + a_2 e^{i\theta} \cdot b_{n-1}. \end{aligned} \tag{2.15}$$

Notice that $h_1 = a_1 e^{i\theta}$ and $h_2 = a_2 e^{i\theta}$ are no longer independent Gaussian distributed even if θ is assumed independent of both a_1 and a_2 . In our analysis, these parameters are assumed to be *unknown constants* during the transmission of a codeword. Nevertheless, in later simulations, a_1 and a_2 will be assumed independent Rayleigh distributed, and θ that is independent of both a_1 and a_2 is uniformly distributed over $[-\pi, \pi)$.



Chapter 3

A Channel with Synchronized Phases Among Channel Taps: The Modified System Model

In this chapter, we will start from Section 3.1, which points out by a simple example that for a blind receiver for QPSK modulations, the phase distortion affects the performance more than the amplitude distortion does. This leads to a straightforward inference that the receiver may need to know the phases in order to yield an acceptable performance. Yet, continuing the discussion along this line, we found that by adding a mild assumption such that the phases among different channel coefficients are synchronized (i.e., identical), the performance of a blind receiver can already be adequately improved even without knowing (estimating) the exact value of these phases. It thus suffices to consider the modified system model introduced in Section 2.4.

Since channel coefficients of the modified system model are no longer independent to each other, some discussion on the statistics of the modified system model becomes necessary, which will be given in Section 3.2. To find the best code design based on the minimization of the union bound, an evaluable formula for the pairwise error rate is needed, which requires an approximate statistics of the modified system model; this is the focus of Section 3.3. We

end this chapter by deriving the optimal blind decoding criterion for the modified system model in Section 3.4.

3.1 Impacts of Phase Distortions and Amplitude Distortions

In this section, we will demonstrate that the phase distortion will affect the performance more than the amplitude distortion does. For simplicity and clarity, we let $P = 1$. Cases with larger P should have similar behavior; hence, we omit them.

First, we consider the case that the phase distortion $\vartheta \triangleq e^{i(\angle h)} = e^{i\theta}$ is unknown while the amplitude distortion $h_m \triangleq |h|$ is known at the receiver, where $h = |h|e^{i\theta} = h_m\vartheta$ is the complex-valued channel coefficient. Since h_m is known at the receiver, the joint maximum-likelihood (JML) decoder becomes

$$(\hat{\mathbf{b}}, \hat{\mathbf{h}}) = \arg \min_{(\mathbf{b}, \vartheta) \in \mathcal{C} \times \mathbb{C}: |\vartheta|=1} \|\mathbf{y} - \mathbb{B}h_m\vartheta\|^2, \quad (3.1)$$

where \mathcal{C} is the set of all codewords, and \mathbb{C} consists of all complex numbers. Denoting the L -by-1 matrix $\mathbb{B}h_m$ by \mathbb{A} , we get

$$\begin{aligned} \|\mathbf{y} - \mathbb{A}\vartheta\|^2 &= (\mathbf{y} - \mathbb{A}\vartheta)^H (\mathbf{y} - \mathbb{A}\vartheta) \\ &= \|\mathbf{y}\|^2 - \mathbf{y}^H \mathbb{A}\vartheta - \vartheta^* \mathbb{A}^H \mathbf{y} + \vartheta^* \mathbb{A}^H \mathbb{A}\vartheta \\ &= \|\mathbf{y}\|^2 - \vartheta \mathbf{y}^H \mathbb{A} - (\vartheta \mathbf{y}^H \mathbb{A})^* + |\vartheta|^2 \mathbb{A}^H \mathbb{A} \\ &= \|\mathbf{y}\|^2 - 2\text{Re} \{ \vartheta \mathbf{y}^H \mathbb{A} \} + \mathbb{A}^H \mathbb{A}. \end{aligned}$$

This results in that

$$\hat{\vartheta} = \arg \min_{\vartheta \in \mathbb{C}: |\vartheta|=1} \|\mathbf{y} - \mathbb{A}\vartheta\|^2$$

should satisfy

$$\hat{\vartheta} \mathbf{y}^H \mathbb{A} = |\mathbf{y}^H \mathbb{A}|.$$

I.e.,

$$\hat{\vartheta} = \frac{\mathbb{A}^H \mathbf{y}}{|\mathbb{A}^H \mathbf{y}|} = \frac{\mathbb{B}^H \mathbf{y}}{|\mathbb{B}^H \mathbf{y}|}. \quad (3.2)$$

Via (3.2), the decoder in (3.1) turns to

$$\begin{aligned} \hat{\mathbf{b}} &= \arg \min_{\mathbf{b} \in \mathcal{C}} \|\mathbf{y} - \mathbb{B}h_m \hat{\vartheta}\|^2 \\ &= \arg \min_{\mathbf{b} \in \mathcal{C}} \left\| \mathbf{y} - \mathbb{B}h_m \frac{\mathbb{B}^H \mathbf{y}}{N h_m} \right\|^2 \end{aligned} \quad (3.3)$$

Next, consider the alternative case that the amplitude distortion h_m is unknown but the phase distortion ϑ is known at the receiver. Similarly, denoting $\mathbb{B}\vartheta$ by \mathbb{D} , we get

$$\begin{aligned} \|\mathbf{y} - \mathbb{D}h_m\|^2 &= (\mathbf{y} - \mathbb{D}h_m)^H (\mathbf{y} - \mathbb{D}h_m) \\ &= \|\mathbf{y}\|^2 - (\mathbf{y}^H \mathbb{D} + \mathbb{D}^H \mathbf{y})h_m + \|\mathbb{D}\|^2 h_m^2. \end{aligned} \quad (3.4)$$

Hence, the estimate of the amplitude distortion, which minimizes (3.4) subject to $h_m > 0$, is given by

$$\begin{aligned} \hat{h}_m &= \left\{ \frac{\mathbf{y}^H \mathbb{D} + \mathbb{D}^H \mathbf{y}}{2\|\mathbb{D}\|^2} \right\}^+ \\ &= \left\{ \frac{\mathbf{y}^H \mathbb{B}\vartheta + \vartheta^* \mathbb{B}^H \mathbf{y}}{2\|\mathbb{B}\vartheta\|^2} \right\}^+ \\ &= \left\{ \frac{e^{i\theta} \mathbf{y}^H \mathbb{B} + e^{-i\theta} \mathbb{B}^H \mathbf{y}}{2N} \right\}^+, \end{aligned} \quad (3.5)$$

where $\{x\}^+ \triangleq \max\{x, 0\}$, and the last step follows from $|\vartheta|^2 = 1$ and $\|\mathbb{B}\|^2 = N$. Following (3.5), we obtain

$$\begin{aligned} \hat{\mathbf{b}} &= \arg \min_{\mathbf{b} \in \mathcal{C}} \|\mathbf{y} - \mathbb{B}\vartheta \hat{h}_m\|^2 \\ &= \arg \min_{\mathbf{b} \in \mathcal{C}} \left\| \mathbf{y} - \frac{1}{2N} \mathbb{B} (e^{i2\theta} \mathbf{y}^H \mathbb{B} + \mathbb{B}^H \mathbf{y}) \right\|^2. \end{aligned} \quad (3.6)$$

With the availability of (3.3) and (3.6), we proceed to compare the resultant performances of the two decoders. Simulation shows that knowing only the amplitude distortion has no

performance gain. In other words, the knowledge of the phase distortion is more critical for a blind receiver. Notably, as will be shown in subsequent chapter, (3.6) will lead to a performance improvement over the criterion in (2.2).

For a practical system, it may be too idealistic to assume that the phase distortion is known or can be accurately estimated at the receiver unless a certain non-trivial implementation cost for channel estimation is permissible. We then found that by assuming that the phases of different channel taps are synchronized as the modified system model has assumed in Section 2.4, an evident improvement over (2.2) can be obtained. This somewhat justifies the necessity of the provision of the modified system model. As aforementioned, the respective decoding criterion for the modified system model will be given in Section 3.4.

3.2 PDFs of the Channel Coefficients of the Modified System Model

In this section, the probability density functions (PDFs) of the channel coefficients of the modified system model introduced in Section 2.4 are discussed.

In this scenario, the simplest case shall be $P = 2$ because we need at least two channel taps to synchronize their phases. Assume that the amplitude distortion h_{m_1} and h_{m_2} are independent Rayleigh distributed with mean $\sqrt{\frac{\pi\tau^2}{2}}$, where $\tau^2 = \frac{\sigma^2}{2}$, and the phase distortion θ is uniformly distributed over $[-\pi, \pi)$ and independent of both h_{m_1} and h_{m_2} . By these assumptions, the marginal PDFs of these parameters can be written as follows.

$$f_{h_{m_1}}(u) = \frac{u}{\tau^2} e^{-\frac{u^2}{2\tau^2}}, \quad u \geq 0$$

$$f_{h_{m_2}}(v) = \frac{v}{\tau^2} e^{-\frac{v^2}{2\tau^2}}, \quad v \geq 0$$

$$f_{\theta}(\theta) = \frac{1}{2\pi}, \quad -\pi \leq \theta \leq \pi$$

When denoting the two channel coefficients as $h_1 = x_1 + iy_1$ and $h_2 = x_2 + iy_2$, we get

$$x_1 = h_{m_1} \cos \theta_1,$$

$$y_1 = h_{m_1} \sin \theta_1,$$

$$x_2 = h_{m_2} \cos \theta_2,$$

$$y_2 = h_{m_2} \sin \theta_2,$$

where $\theta_1 = \theta_2 = \theta$ with probability one. By the independence of h_{m_1} , h_{m_2} and θ , we derive

$$f_{h_1, h_2}(ue^{i\theta_1}, ve^{i\theta_2}) = f_{h_{m_1}, h_{m_2}, \theta_1, \theta_2}(u, v, \theta_1, \theta_2) = \frac{u}{\tau^2} e^{-\frac{u^2}{2\tau^2}} \cdot \frac{v}{\tau^2} e^{-\frac{v^2}{2\tau^2}} \cdot \frac{1}{2\pi} \delta(\theta_1 - \theta_2). \quad (3.7)$$

Through the Jacobian transformation, we get

$$f_{x_1, y_1, x_2, y_2}(x_1, y_1, x_2, y_2) = \frac{1}{2\pi\tau^4} e^{-\frac{x_1^2 + y_1^2 + x_2^2 + y_2^2}{2\tau^2}} \delta\left(\tan \frac{y_1}{x_1} - \tan \frac{y_2}{x_2}\right). \quad (3.8)$$

Since (3.8) does not lead to a close-form formula for the pair-wise error rate for the modified system model in Section 2.4, we will seek an approximate to it in the next section.

3.3 Approximate PDFs of the Channel Coefficients of the Modified System Model

When the channel coefficients are zero-mean independent Gaussian distributed, the pairwise error rate exhibits a close-form expression as have been derived in (2.14). In order to use this close-form expression, a zero-mean Gaussian approximate \mathbf{f}_{h_1, h_2} to (3.8) is needed.

A straightforward approximate to f_{h_1, h_2} in (3.7) is to make the zero-mean independent Gaussian \mathbf{f}_{h_1, h_2} having the same covariance matrix as f_{h_1, h_2} . We then derive based on f_{h_1, h_2}

that

$$\begin{aligned}
E[h_1 h_2^*] &= \int_{\mathbb{C}} \int_{\mathbb{C}} ab^* f_{h_1, h_2}(a, b) da db \\
&= E[h_{m_1} \cdot e^{j\theta} \cdot h_{m_2} \cdot e^{-j\theta}] \\
&= E[h_{m_1} \cdot h_{m_2}] \\
&= E[h_{m_1}] E[h_{m_2}];
\end{aligned} \tag{3.9}$$

hence, the covariance matrix due to f_{h_1, h_2} is given by

$$\mathbb{S}_h = \begin{bmatrix} \sigma^2 & \frac{\pi\sigma^2}{4} \\ \frac{\pi\sigma^2}{4} & \sigma^2 \end{bmatrix}. \tag{3.10}$$

Accordingly, we adopt $\mathbf{f}_{h_1, h_2} \sim N(0, \mathbb{S}_h)$ as the approximate PDF to f_{h_1, h_2} .

Since the pairwise error probability (PEP) in Section 2.2 is determined by the statistics of X_n , we examine how well \mathbf{f}_{h_1, h_2} approximate f_{h_1, h_2} by analyzing the moments of X_n in the sequel. Apparently, the second moments of X_n due to both f_{h_1, h_2} and \mathbf{f}_{h_1, h_2} are the same. We then proceed to compare the fourth moment of X_n .

From [5], an elementary result for a zero-mean complex Gaussian random variable Z is that

$$E[Z^{2m}] = m! \cdot E^m[|Z|^2].$$

Therefore, the fourth moment of X_n from (2.10) with respect to the zero-mean Gaussian \mathbf{f}_{h_1, h_2} is

$$E[X_n^4] = 2, \tag{3.11}$$

since $E[X_n] = 0$ and $E[X_n^2] = 1$ under PDF \mathbf{f}_{h_1, h_2} . The fourth moment of X_n with respect to f_{h_1, h_2} however does not have a close-form formula. Thus, we numerically obtain it via Monte Carlo simulation and summarize the results in Figure 3.1.

We can then conclude from the figure that the fourth moments of the precise f_{h_1, h_2} and the approximate \mathbf{f}_{h_1, h_2} are almost equal for $N = 4, 6$ and 8 . Therefore, the PEP formula

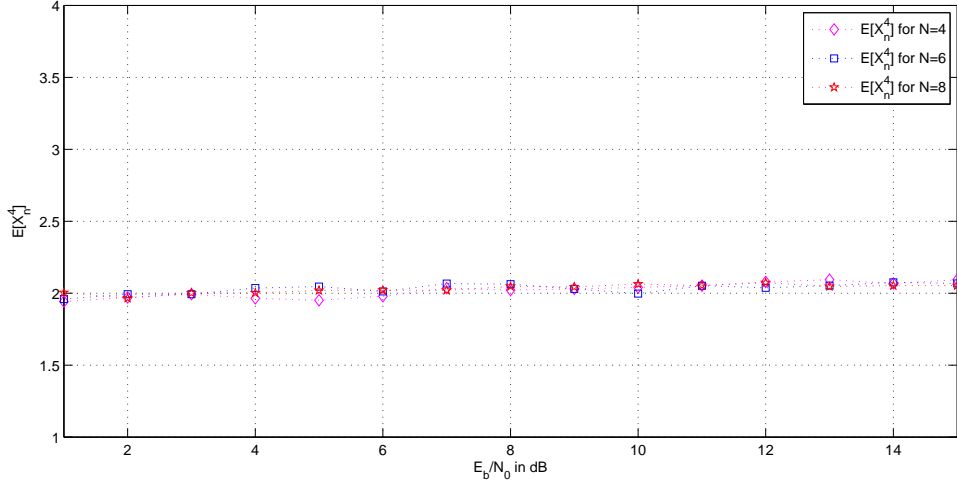


Figure 3.1: $E[X_n^4]$ with respect to f_{h_1, h_2} via Monte Carlo simulation.

derived in Section 2.2 should be a good approximate to the true PEP when the precise PDF f_{h_1, h_2} of the channel coefficients are used.

3.4 The Decoding Criterion of the Modified System Model

We end this chapter by providing the optimal decoding criterion for the modified system model.

Consider without loss of generality the case of $P = 2$. The channel coefficient vector $\mathbf{h} = [h_1 \ h_2]^T$ of the modified system model is given by

$$\mathbf{h} = \mathbf{h}_m \vartheta, \quad (3.12)$$

where $\mathbf{h}_m = [h_{m_1} \ h_{m_2}]^T$ is amplitude distortion vector and $\vartheta \triangleq e^{i(\angle h_1)} = e^{i(\angle h_2)}$ is phase distortion.

By the formula below,

$$\begin{aligned} \min_{(\mathbf{b}, \mathbf{h}) \in \mathcal{C} \times \mathbb{C}^P} \|\mathbf{y} - \mathbb{B}\mathbf{h}\|^2 &= \min_{(\mathbf{b}, \mathbf{h}_m, \vartheta) \in \mathcal{C} \times \mathbb{C}^2 \times [-\pi, \pi]: \mathbf{h}_m \geq 0} \|\mathbf{y} - \mathbb{B}\mathbf{h}\|^2 \\ &= \min_{\mathbf{b} \in \mathcal{C}} \min_{\mathbf{h}_m \in \mathbb{C}^2: \mathbf{h}_m \geq 0} \min_{\vartheta \in [-\pi, \pi]} \|\mathbf{y} - \mathbb{B}\mathbf{h}\|^2, \end{aligned}$$

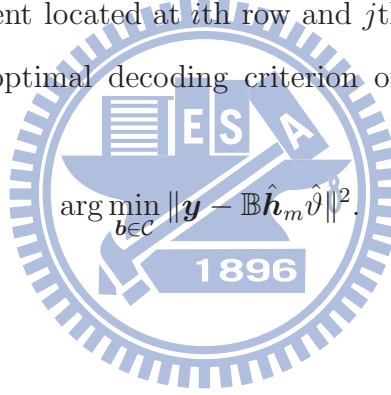
we can find the minimizers for \mathbf{h}_m and ϑ in sequence as follows.

$$\begin{aligned} \hat{\vartheta} &= (\mathbf{h}_m^H \mathbb{B}^H \mathbb{B} \mathbf{h}_m)^{-1} \mathbf{h}_m^H \mathbb{B}^H \mathbf{y}, \\ \hat{h}_{m_1} &= \left\{ \sum_{n=1}^L (y_n^* g_{n,1} + y_n g_{n,1}^*) - \hat{h}_{m_2} \sum_{n=1}^L (g_{n,1} g_{n,2}^* + g_{n,1}^* g_{n,2}) \right\} / N, \\ \hat{h}_{m_2} &= \left\{ \sum_{n=1}^L (y_n^* g_{n,2} + y_n g_{n,2}^*) - \hat{h}_{m_1} \sum_{n=1}^L (g_{n,1} g_{n,2}^* + g_{n,1}^* g_{n,2}) \right\} / N, \end{aligned}$$

where $g_{i,j}$ represents the element located at i th row and j th column of the matrix $\mathbb{G} = \mathbb{B}\hat{\vartheta}$.

With these minimizers, the optimal decoding criterion of the modified system model is straightforwardly given by

$$\arg \min_{\mathbf{b} \in \mathcal{C}} \|\mathbf{y} - \mathbb{B}\hat{\mathbf{h}}_m \hat{\vartheta}\|^2.$$



Chapter 4

The Simulation Results

In this chapter, we will illustrate the simulation results in Section 4.1, and remarked them in Section 4.2.

4.1 System Settings

In this section, we present the performances of codes designed in the previous chapters.

In our simulations, other than the requirement that the channel taps satisfy $E[\mathbf{h}\mathbf{h}^H] = (1/P)\mathbb{I}_P$, where \mathbb{I}_P denotes the P -by- P identity matrix, we will focus on three kinds of channel setting:

1. The channel is a Rayleigh-fading channel with $P = 1$.
2. The channel is a Rayleigh-fading channel with $P = 2$, in which \mathbf{h} is a zero-mean, independent and identically distributed complex Gaussian random vector. Note that in this setting, the phases of the two channel taps are independent. This system model is the same as the one used in [1] and [4].
3. The channel is the one we have mentioned in Section 2.4. The channel taps \mathbf{h} becomes dependent because the phases of the two channel taps are required to be the same.

The amplitude of \mathbf{h} remains independent.

Three kinds of decoders will be examined in our simulations:

1. The decoder does not know both the amplitude distortions and the phase distortions.
2. The decoder does not know the amplitude distortions but knows the phase distortions.
3. The decoder does not know the phase distortions but knows the amplitude distortions.
4. The decoder does not know the amplitude distortions and the phase distortions, but knows that phases distortions are synchronized.

Figures 4.1–4.4 use codes designed in Sections 2.2 and 2.3. Figures 4.1 and 4.2 (respectively, Figures 4.3 and 4.4) illustrate the performances of the first, the second decoders, and the third decoders for codes based on BPSK (respectively, QPSK) modulations that are transmitted over the first channel model, i.e., $P = 1$.

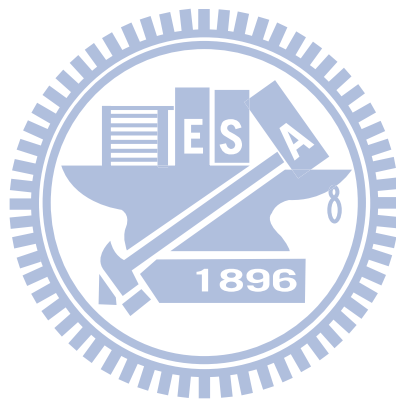
Figures 4.5–4.8 give the performances of codes designed for the second system model, i.e. $P = 2$. Likewise, Figures 4.5 and 4.6 (respectively, Figures 4.7 and 4.8) show the performances of the first and the second decoders for codes based on BPSK (respectively, QPSK) modulations.

Figures 4.9 and 4.10 compare the BPSK-based and QPSK-based codes, which are designed for and transmitted over the second $P = 2$ system model but decoded using the second decoder.

Figures 4.11 and 4.12 compare the BPSK-based and QPSK-based codes, which are designed for the third $P = 2$ system model but are transmitted over the third $P = 2$ channel. The decoder in these two figures is the third one.

The above figures consider only the half rate codes. For different code rates respectively

for BPSK-based and QPSK-based codes, the performances are summarized in Figures 4.13 and 4.14.



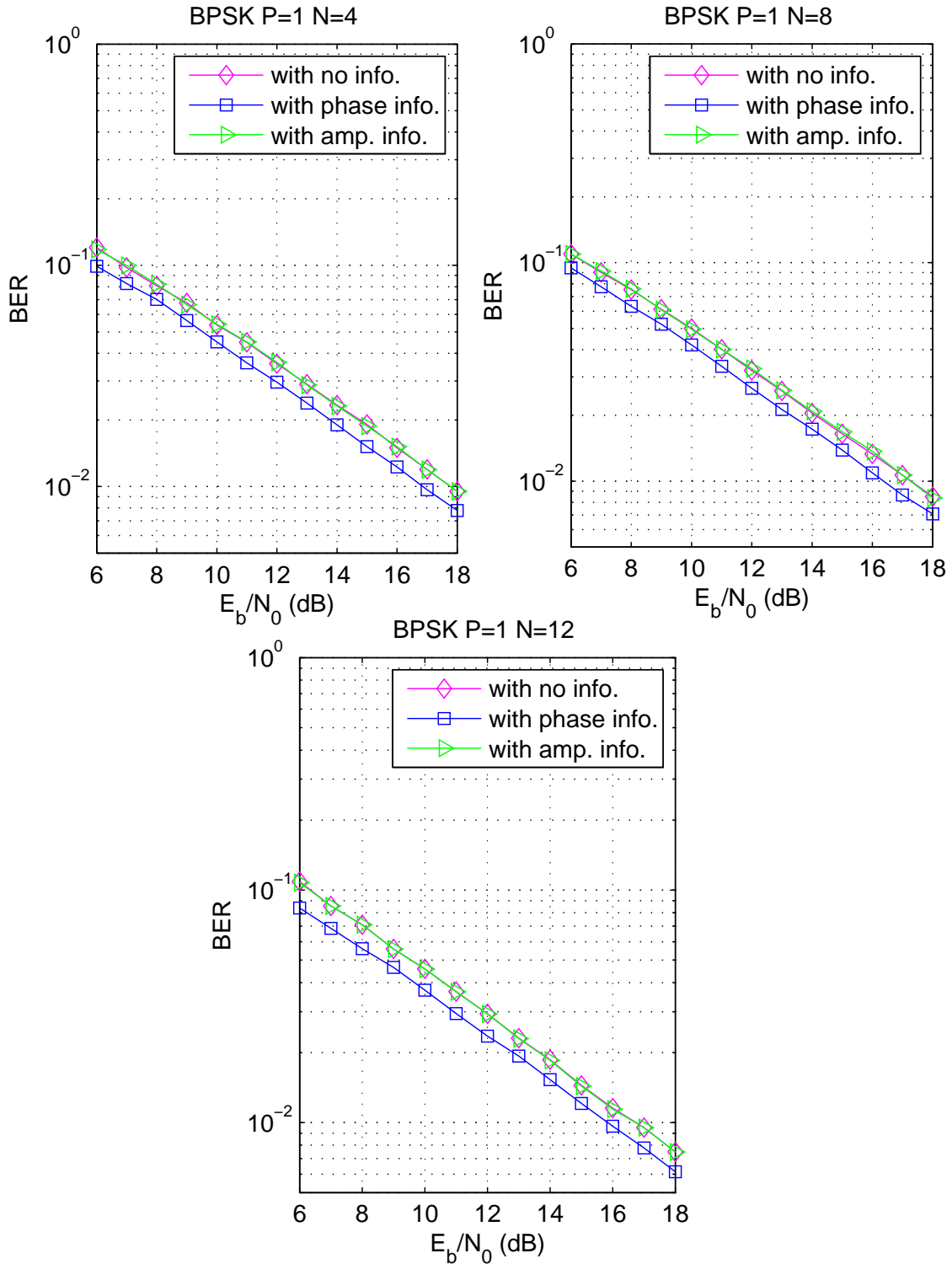


Figure 4.1: The BERs of BPSK-modulated codes using decoder with no/phase/amplitude distortion information. The channel simulated is the Rayleigh-fading channel with $P = 1$. Here, the codeword lengths examined are $N = 4, 8, 12$, respectively.

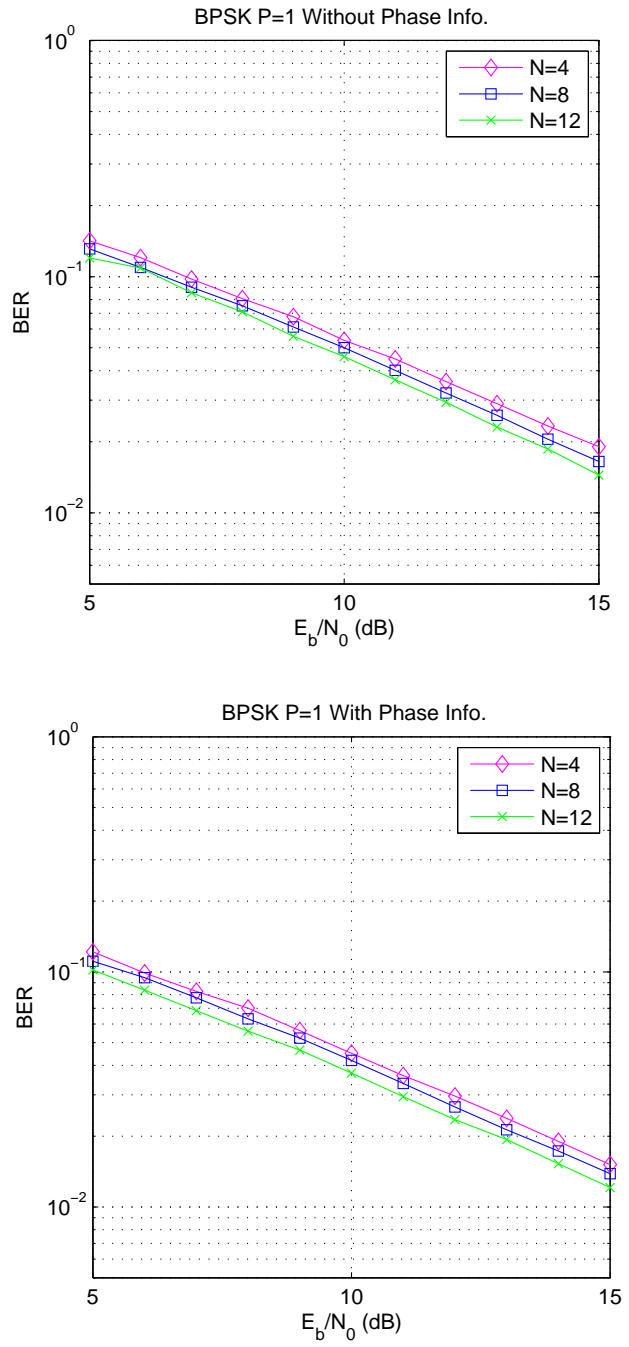


Figure 4.2: The BERs of BPSK-modulated codes using decoder without/with phase distortion information. The channel simulated is the Rayleigh-fading channel with $P = 1$. Here, the codeword lengths examined are 4, 8, 12.

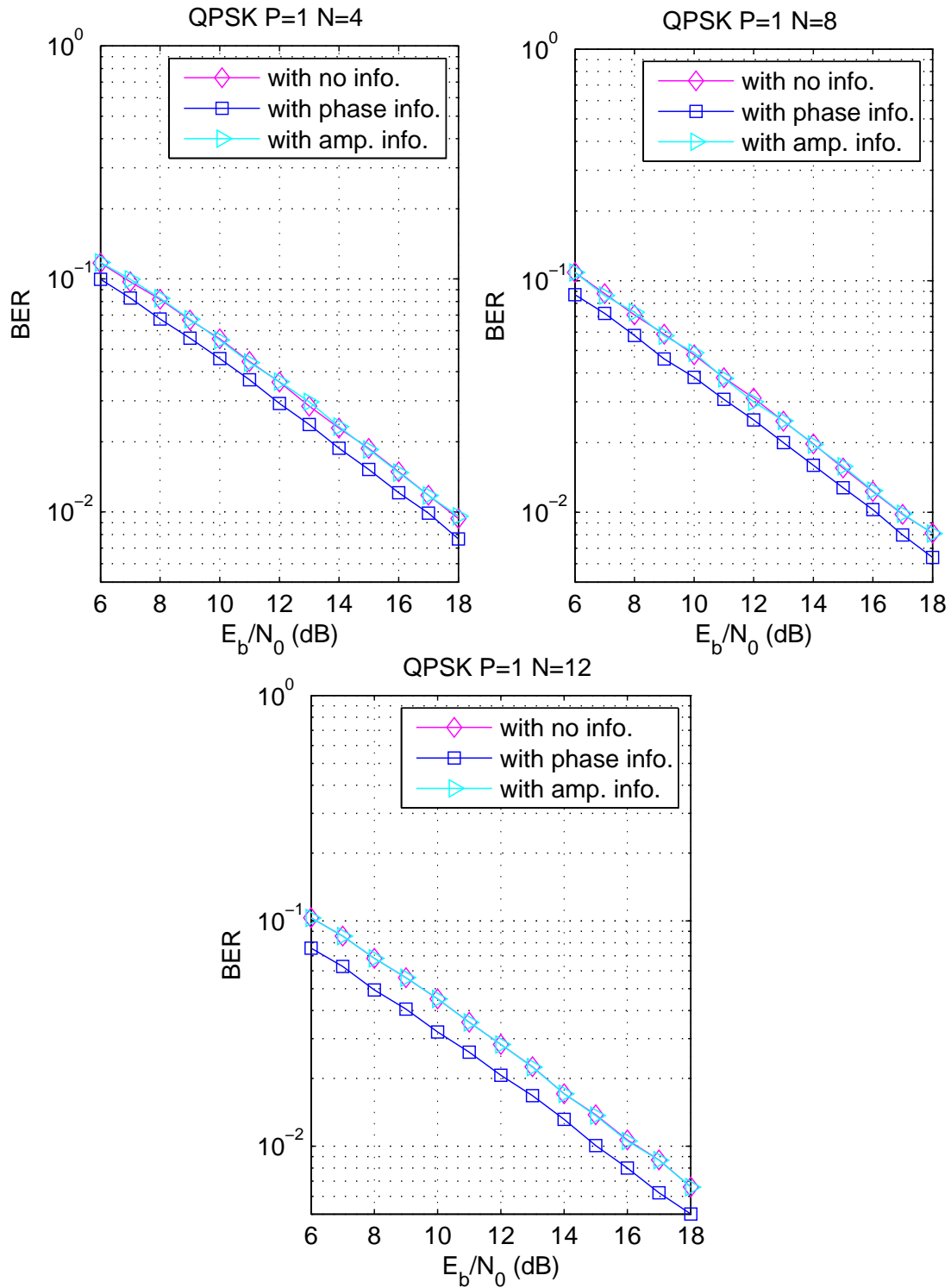


Figure 4.3: The BERs of QPSK-modulated codes using decoder with no/phase/amplitude phase distortion information. The channel simulated is the Rayleigh-fading channel with $P = 1$. Here, the codeword lengths examined are $N = 4, 8, 12$.

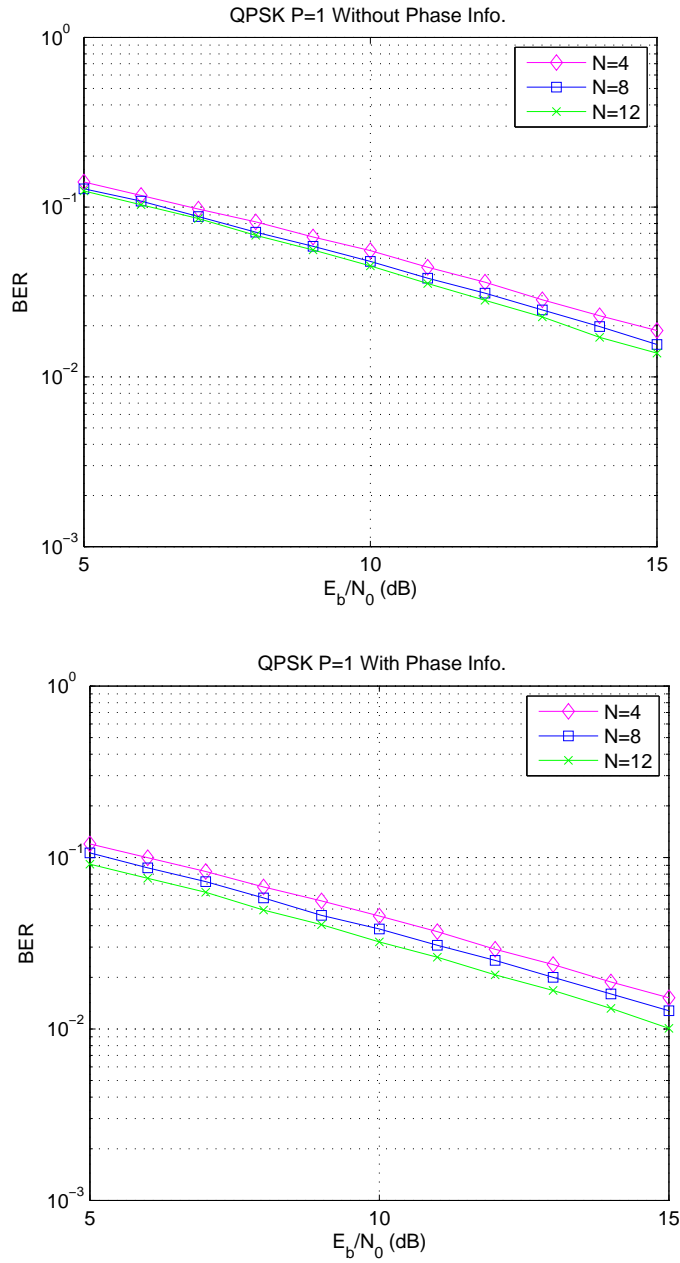


Figure 4.4: The BERs of QPSK-modulated codes using decoder without/with phase distortion information. The channel simulated is the Rayleigh-fading channel with $P = 1$. Here, the codeword lengths examined are $N = 4, 8, 12$.

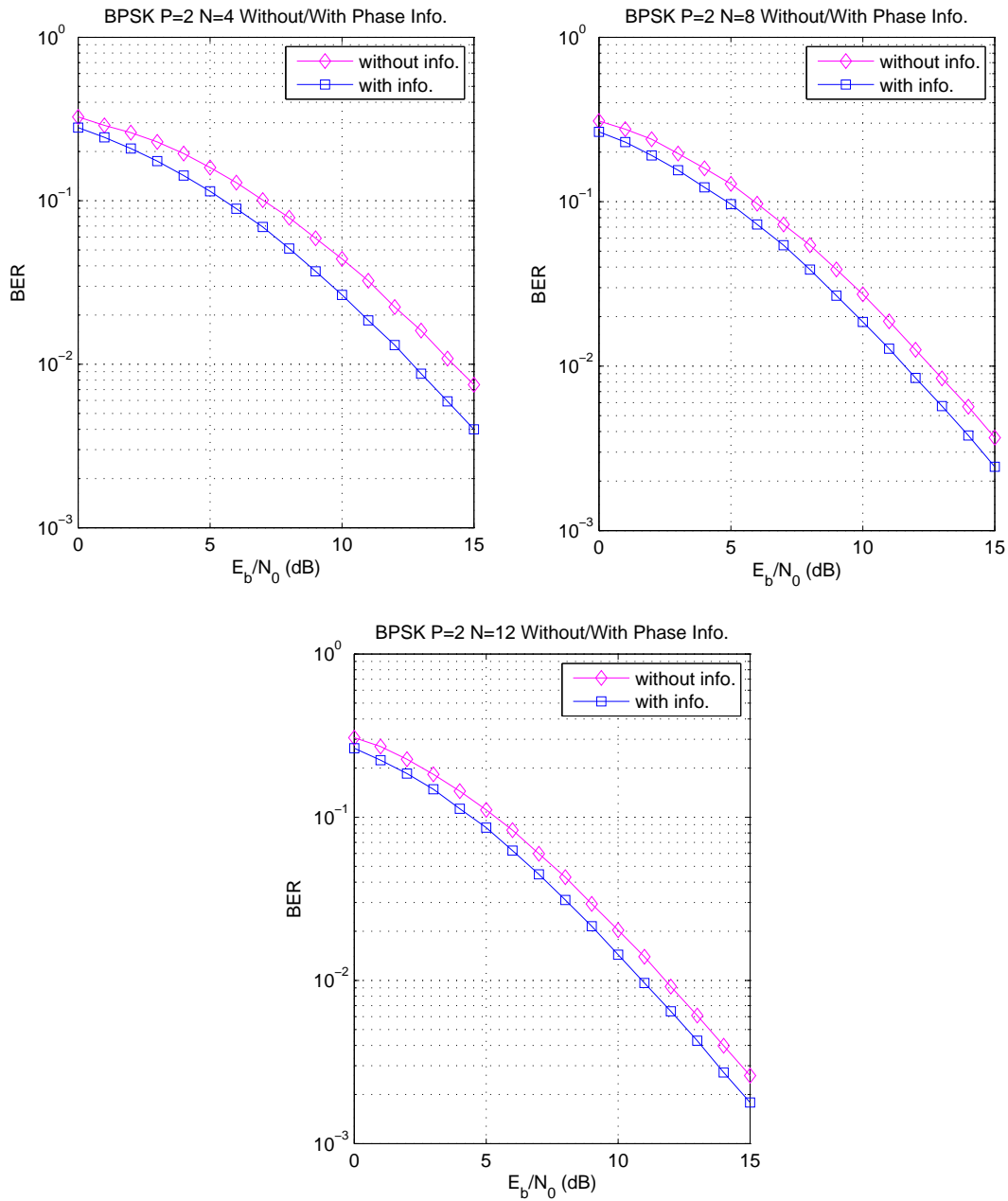


Figure 4.5: The BERs of BPSK-modulated codes using decoder without/with phase distortion information. The channel simulated is the multi-path Rayleigh-fading channel with $P = 2$. Here, the codeword lengths examined are $N = 4, 8, 12$.

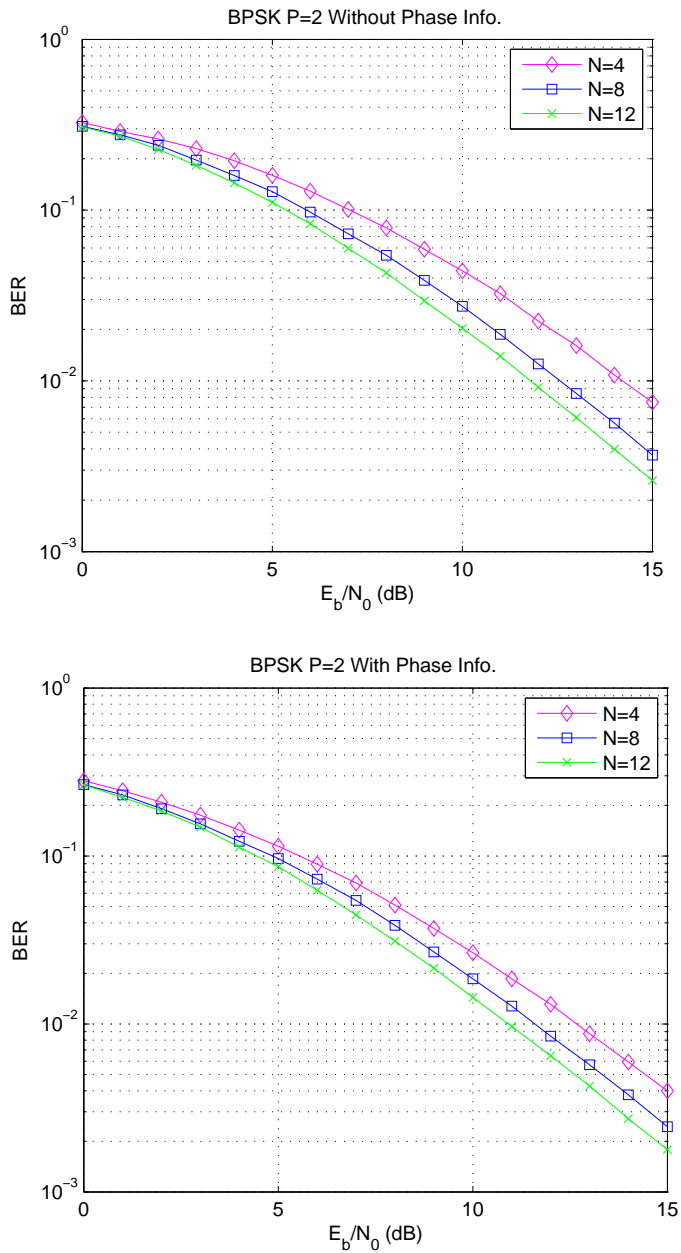


Figure 4.6: The BERs of BPSK-modulated codes using decoder without/with phase distortion information. The channel simulated is the multi-path Rayleigh-fading channel with $P = 2$. Here, the codeword lengths examined are $N = 4, 8, 12$.

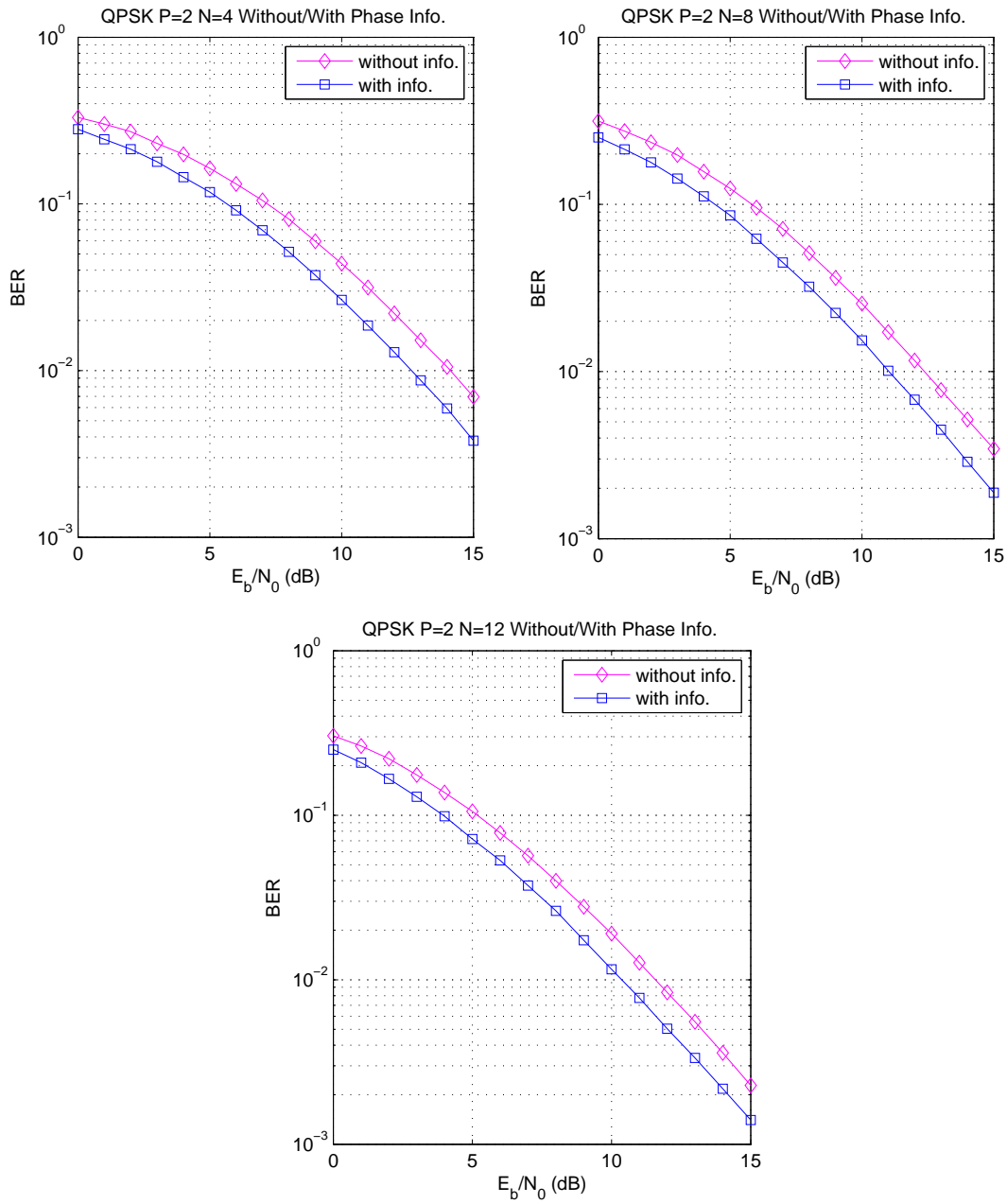


Figure 4.7: The BERs of QPSK-modulated codes using decoder without/with phase distortion information. The channel simulated is the multi-path Rayleigh-fading channel with $P = 2$. Here, the codeword lengths examined are $N = 4, 8, 12$.

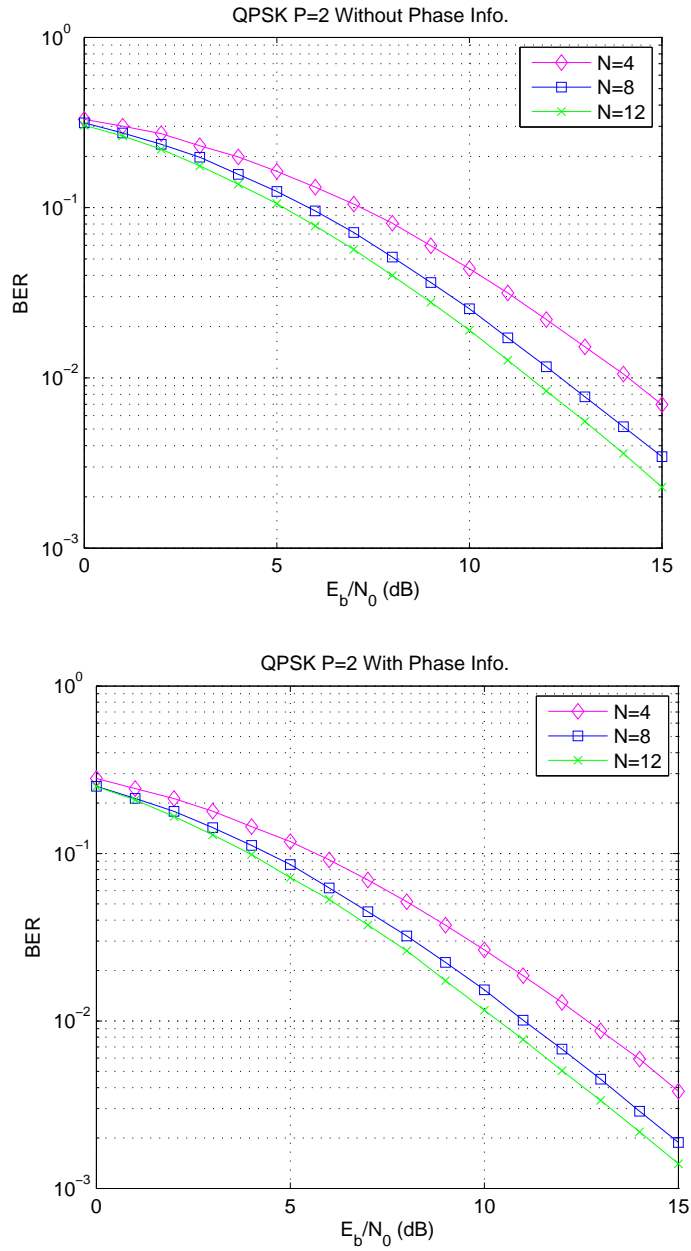


Figure 4.8: The BERs of QPSK-modulated codes using decoder without/with phase distortion information. The channel simulated is the multi-path Rayleigh-fading channel with $P = 2$. Here, the codeword lengths examined are $N = 4, 8, 12$.

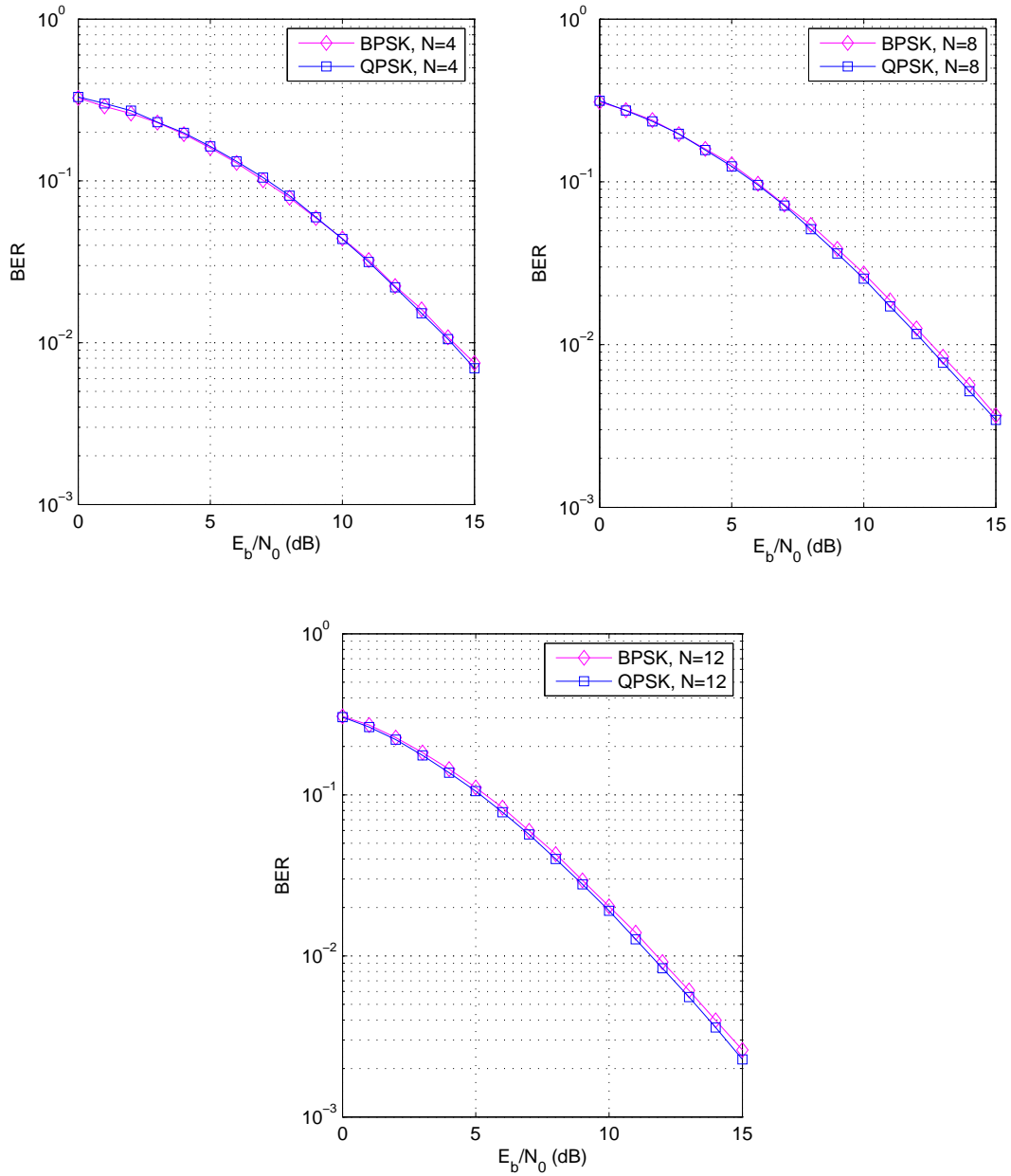


Figure 4.9: The BERs of BPSK-modulated and QPSK-modulated codes using decoder without any information on the channels. The channel simulated is the multi-path Rayleigh-fading channel with $P = 2$, for which the phases of two channel taps are independent. Here, the codeword lengths examined are $N = 4, 8, 12$.

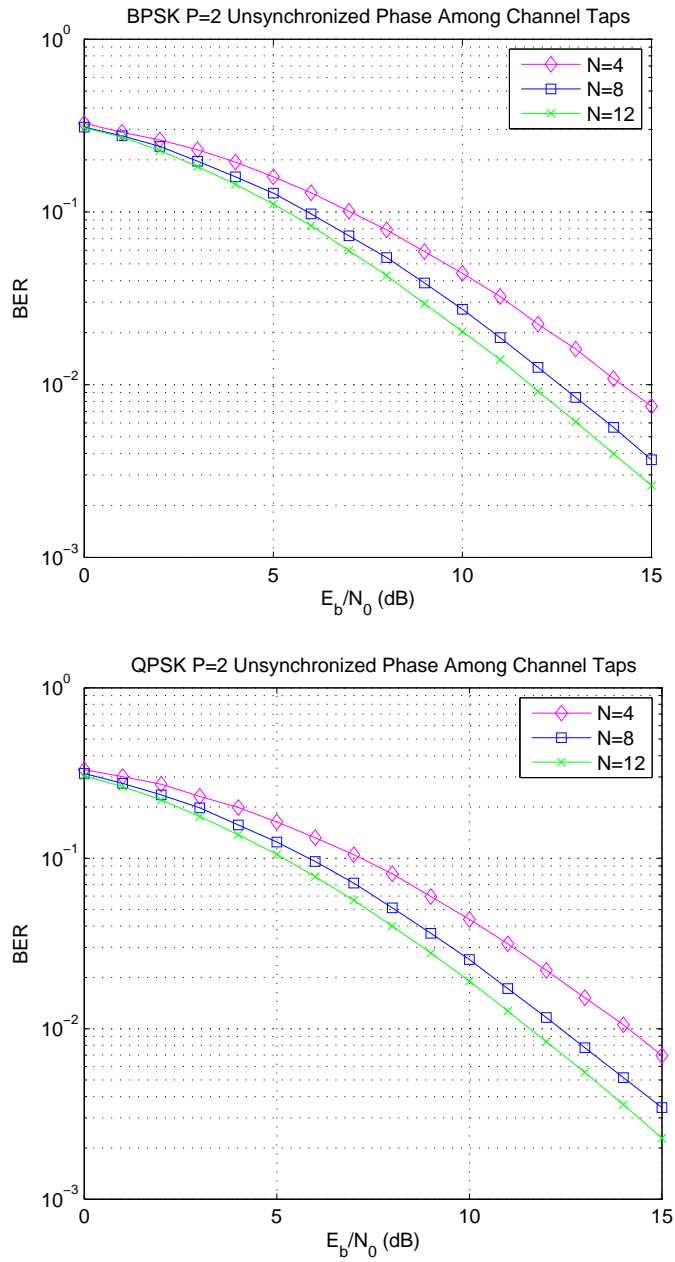


Figure 4.10: The BERs of BPSK-modulated and QPSK-modulated codes using decoder without any information on the channels. The channel simulated is the multi-path Rayleigh-fading channel with $P = 2$, for which the phases of two channel taps are independent. Here, the codeword lengths examined are $N = 4, 8, 12$.

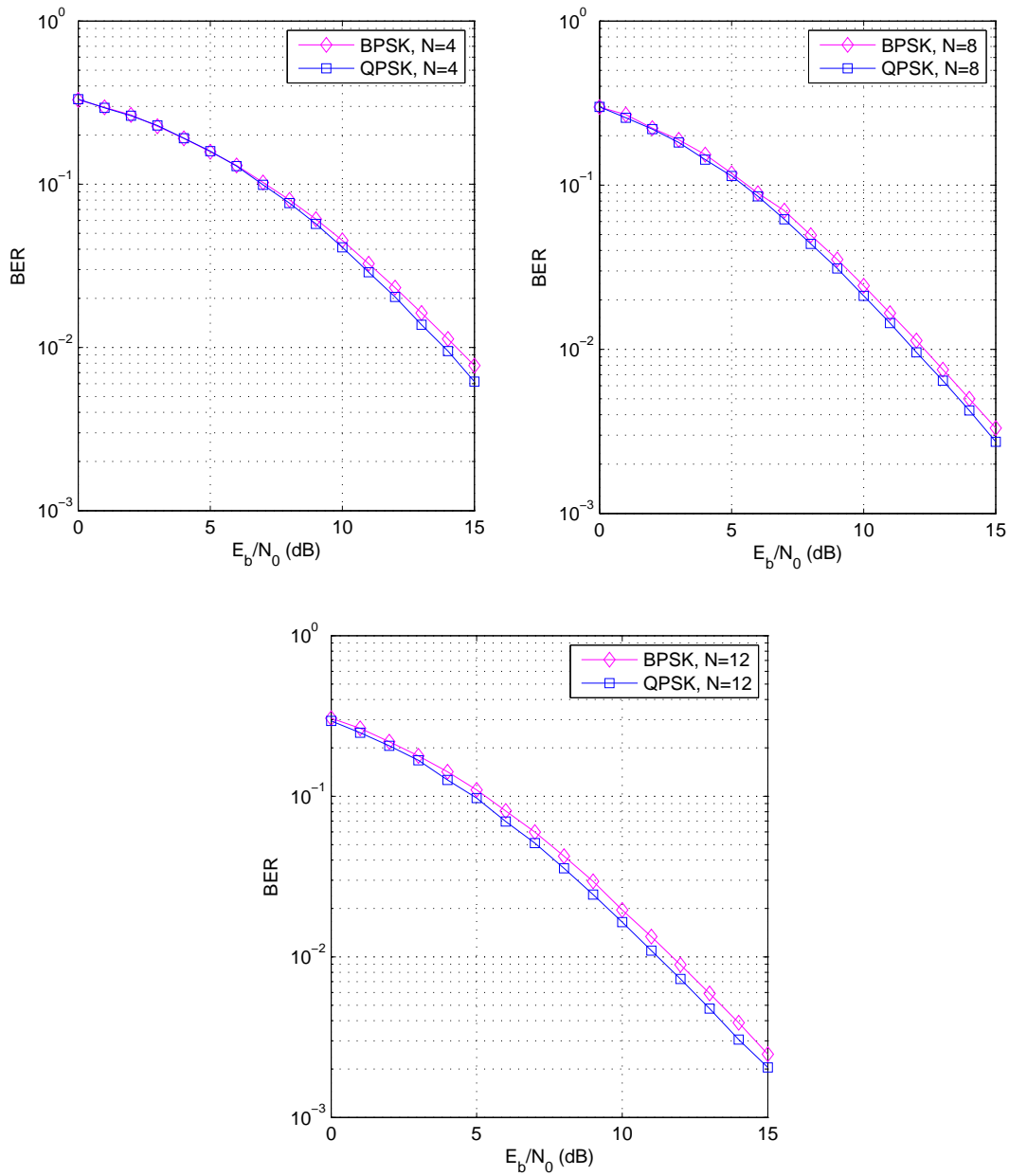


Figure 4.11: The BERs of BPSK-modulated and QPSK-modulated codes using decoder with the information that the phases of two channel taps are synchronized. The channel simulated is the multi-path fading with $P = 2$, for which the phases of two channel taps are also synchronized. Here, the codeword lengths examined are $N = 4, 8, 12$.

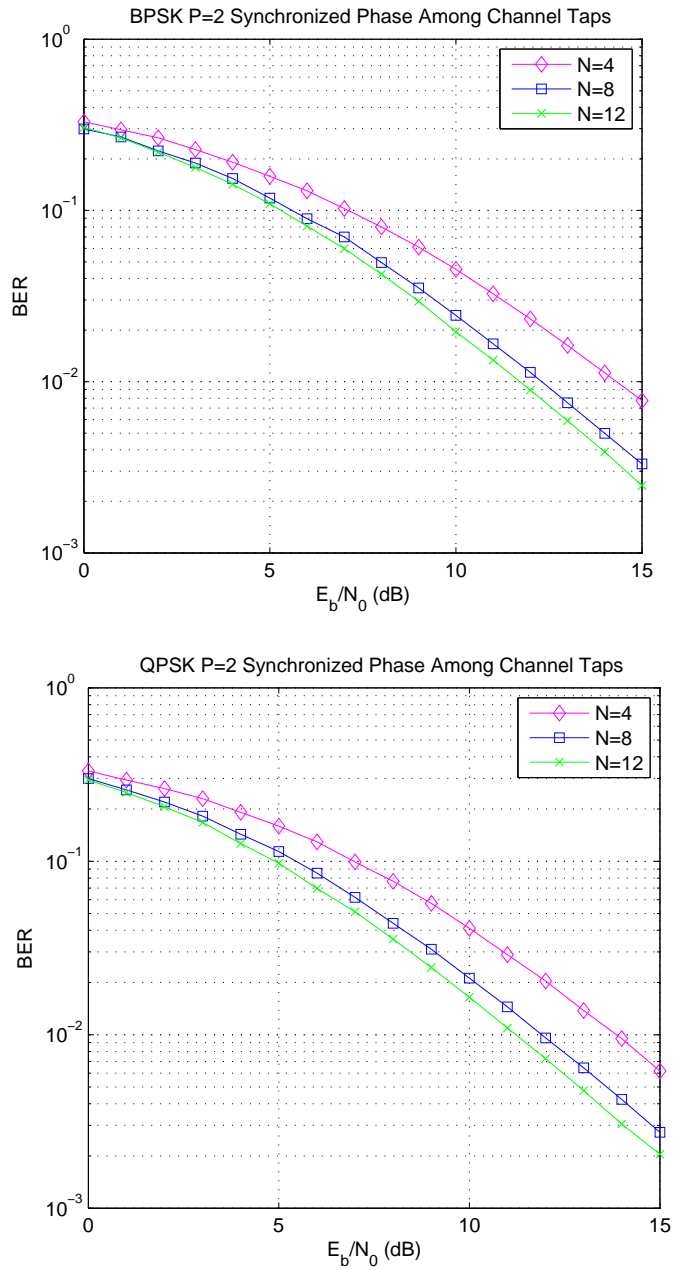


Figure 4.12: The BERs of BPSK-modulated and QPSK-modulated codes using decoder with the information that the phases of two channel taps are synchronized. The channel simulated is the multi-path fading with $P = 2$, for which the phases of two channel taps are also synchronized. Here, the codeword lengths examined are $N = 4, 8, 12$.

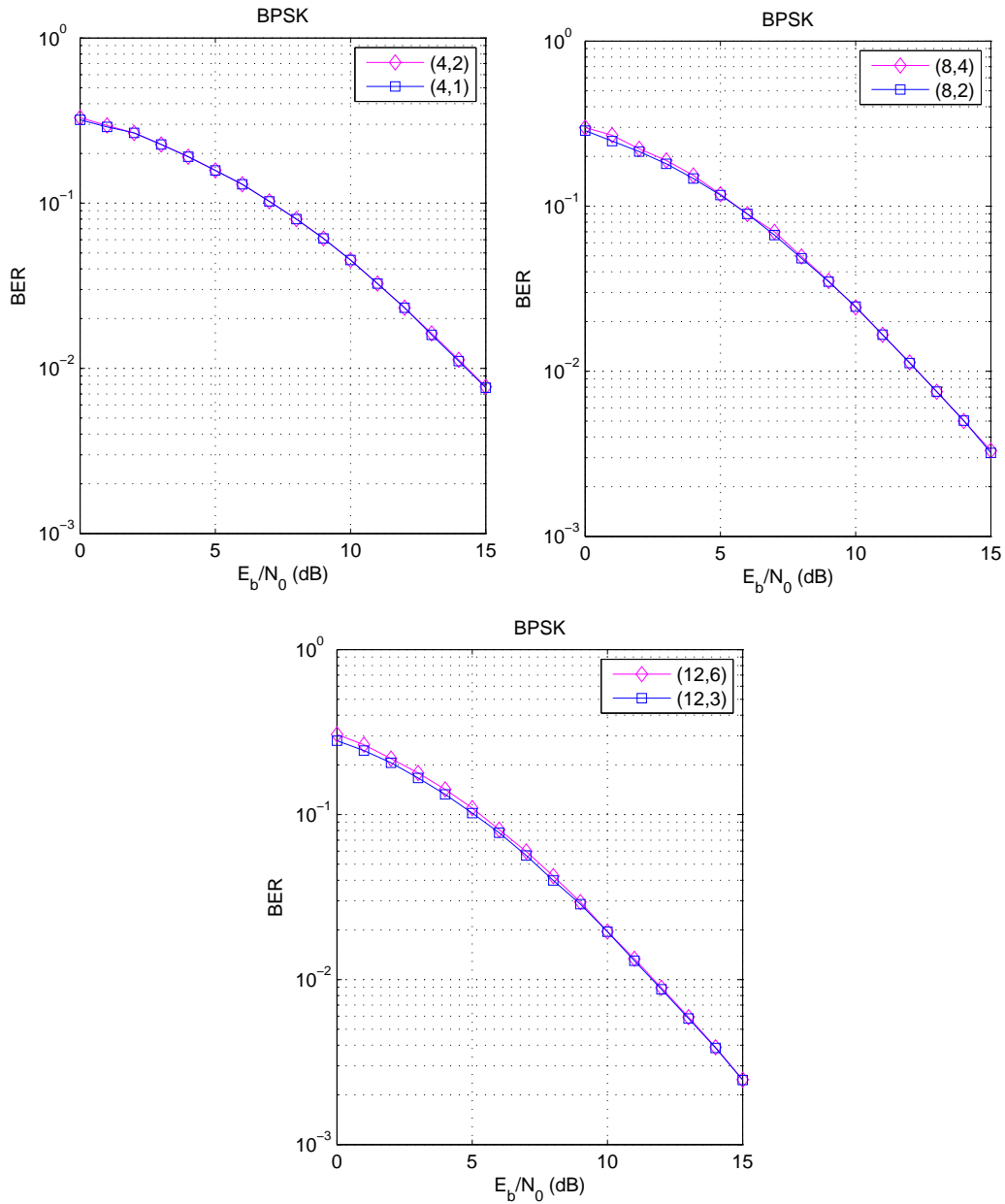


Figure 4.13: The BERs of the $(N, N/2)$ and $(N, N/4)$ BPSK-modulated codes using decoder with the information that the phases of two channel taps are synchronized. The channel simulated is the multi-path fading with $P = 2$, for which the phases of two channel taps are also synchronized. Here, the codeword lengths examined are $N = 4, 8, 12$.

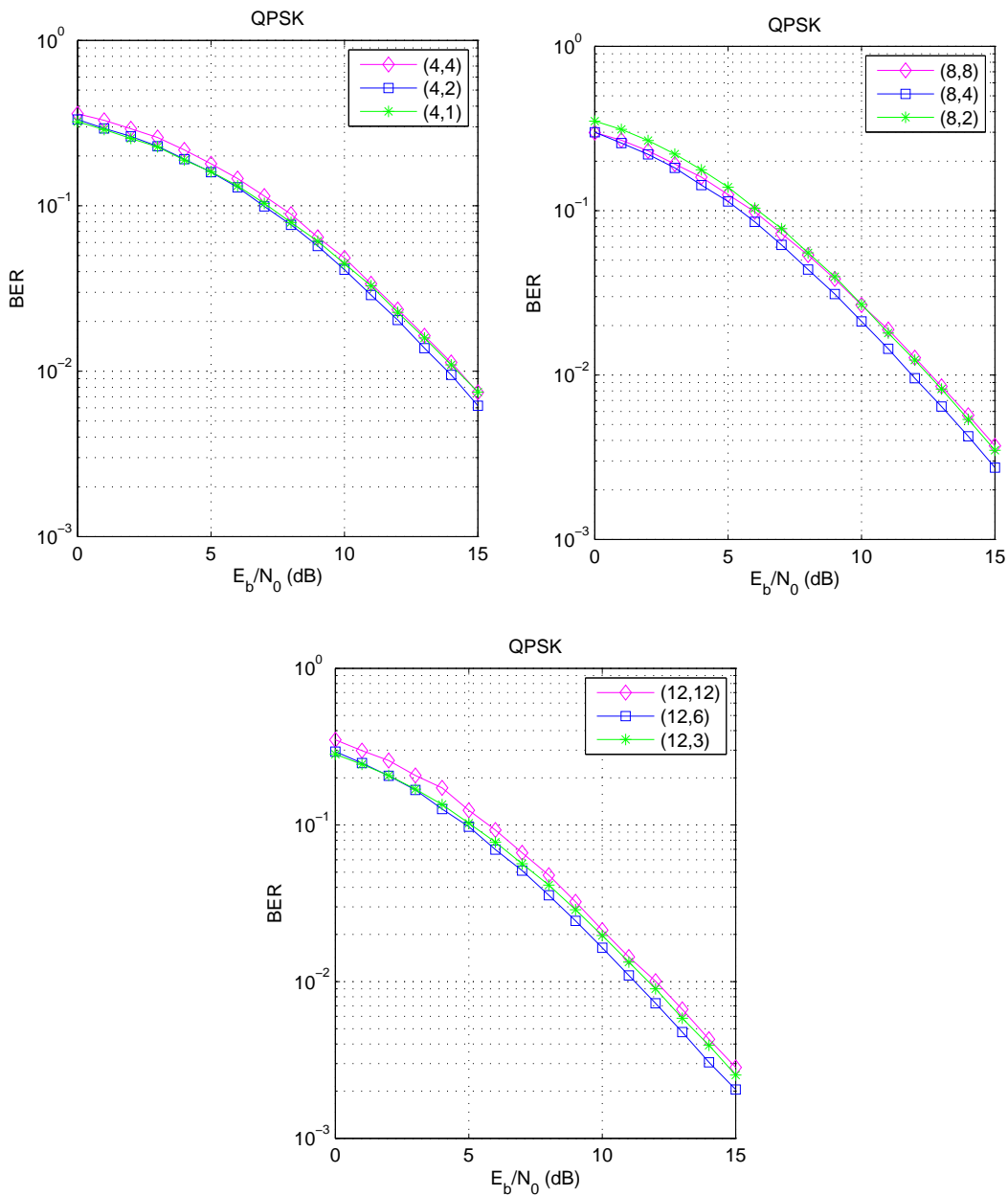


Figure 4.14: The BERs of the (N, N) , $(N, N/2)$, $(N, N/4)$ QPSK-modulated codes using decoder with the information that the phases of two channel taps are synchronized. The channel simulated is the multi-path fading with $P = 2$, for which the phases of two channel taps are also synchronized. Here, the codeword lengths examined are $N = 4, 8, 12$.

4.2 General Remarks

Figures 4.1, 4.3, 4.5 and 4.7 clearly illustrate that knowing the phase information at the receiver can yield evident performance gain, but knowing the amplitude information at the receiver yield no gain. For example, it can be seen from Figures 4.1 and 4.3 that when N is fixed as 12, we can obtain respectively 1 dB and 1.2 dB performance gain by providing phase information to the receiver at $\text{BER}=10^{-2}$. When the channel becomes of two paths, the performance gains are reduced down to 0.8 and 1 dB as shown from Figures 4.5 and 4.7, respectively. A side observation is that QPSK-modulated codes will yield a little more performance gain than BPSK-modulated codes when the phase information is additionally provided to the receiver.

Next, we compare the performance differences between BPSK and QPSK modulated codes when the codes are transmitted over the Rayleigh fading channel (Figure 4.9) and its corresponding modified channel model (Figure 4.11) in which the phases of different channel taps are assumed to be synchronized. By considering the codeword length $N = 12$ and channel memory order $P = 2$, the performance difference is about 0.2 dB at $\text{BER}=10^{-2}$ in Figure 4.9, and about 0.5 dB at $\text{BER}=10^{-2}$ in Figure 4.11. This infers that when the phases of the channel taps are synchronized, QPSK modulation is more favored.

Finally, we examine the performances of codes with different code rates in Figures 4.13 and 4.14. By fixing the energy possessed by each information bit, we obtain that $(N, N/2)$ codes have the best performance. The reasons are as follows. For code rates smaller than one half, each code bit may have insufficient energy to combat noises, which degrades the performance. For code rates larger than one half, the “distance” between \mathbb{P}_B pairs decreases; hence, the performance is also getting worse.

Chapter 5

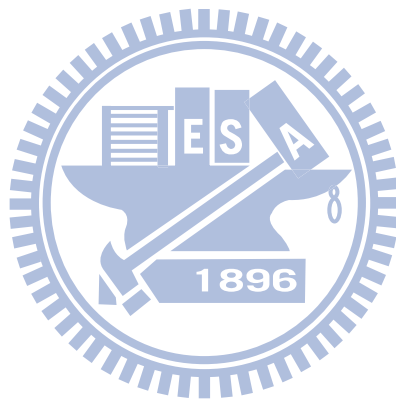
Conclusion Remarks and Future Work

In this thesis, we derived an approximation close-form formula for the union bound of the error performance for QPSK-modulated codes transmitted over a frequency-selective fading channel and demodulated by a blind receiver. Based on the criterion, we then searched for good QPSK-modulated codes for combined channel estimation and error protection by computers. Simulations however show that the blind receiver of QPSK-modulated codes may need to know the phase information of the channel taps in order to obtain an acceptable coding gain over the BPSK-modulated codes.

By adding a simple assumption that phases among different channel taps are synchronized even if they are unknown, a significant improvement in performance can then be observed. To be specific, our simulations show that QPSK-modulated codes perform 0.5 dB better than BPSK-modulated codes when $\text{BER} = 10^{-2}$ and codeword length $N = 12$.

Several issues can be further studied. The first one is to find a systematic code design for our simulated-annealing-based computer-searched codes. The second issue is to establish a decoding scheme for such codes with low decoding complexity. Other than these two, further analysis of the bizarre effect of code rates as have been reported in Section 4.2 could also be worth of further study. Extensions of the QPSK modulations to QAM modulation in order

to increase the transmission rate should be a good next step along this research line.



Bibliography

- [1] M. Skoglund, J. Giese and S. Parkvall, “Code design for combined channel estimation and error protection,” *IEEE Trans. Inform. Theory*, vol. 48, no. 5, pp. 1162-1171, May 2002.
- [2] S. Kirkpatrick, Jr. C. D. Gelatt, and M.P. Vecchi, “Optimization by simulation annealing,” *Science*, vol. 220, no. 4598, pp. 671-680, 1983.
- [3] J. P. Imhof, “Computing the distribution of quadratic forms in normal variables,” *Biometrika*, vol. 48, no. 3-4, pp. 419-426, 1961.
- [4] C.-L. Wu, P.-N. Chen, Yunghsiang S. Han and M.-Hsin Kuo, “Maximum-likelihood priority-first search decodable codes for combined channel estimation and error protection,” *IEEE Trans. Inform. Theory*, vol. 55, no. 9, pp. 4191-4203, Sept. 2009.
- [5] I.S. Reed, “On a moment theorem for complex Gaussian processes,” *IRE Trans. Inform. Theory*, vol. IT-8, pp. 194-195, Apr. 1962.